Rubble stone masonry walls – Evaluation of shear strength by diagonal compression tests

Jelena Milosevic [1], António S. Gago[2], Mário Lopes[3], Rita Bento[4]

ABSTRACT

In Lisbon and other southern European cities, old masonry buildings are generally exposed to a very high seismic risk due to high probability of earthquake occurrence. In order to preserve this architectural heritage and reduce the seismic risk, structural studies should be conducted to decide where and how strengthening techniques should be used. However, to obtain reliable results the structural models should be based on experimental results. This paper describes experimental and numerical studies carried to characterize the shear strength of rubble stone masonry walls. The described work was done within the scope of the research project Seismic Vulnerability of Old Masonry Buildings (www.severes.org). For the experimental program four rubble stone masonry walls (120cm×120cm×70cm) were built using traditional techniques and materials. Two types of mortar were used: air lime mortar (in two masonry specimens) and hydraulic lime mortar (in the other two specimens). The specimens were tested under diagonal compression to evaluate the shear strength of rubble stone masonry. From the tests results it was obtained for the two types of masonry (rubble stone masonry with air or with hydraulic lime mortar) the resistance in the absence of axial compression (cohesion) and the shear modulus. The experimental tests were also simulated by nonlinear finite element models and distinct element models, which provided calibration data for numerical models. The numerical models and its results, which showed a good agreement with the experimental data, are presented in the paper, as well as, some conclusions about numerical modeling strategies.

Keywords: Rubble masonry walls, Diagonal compression test, Shear strength, Cohesion, Finite element model, Distinct element model

1. INTRODUCTION

In Lisbon and other southern European cities, old masonry buildings are generally exposed to a very high seismic risk due to high probability of earthquake occurrence. To reduce the seismic risk of old masonry buildings different strengthening techniques must be implemented to increase, simultaneously, the strength and the ductility of the masonry walls, the rigidity of the wood pavements and the strength of the connections "pavements-masonry walls". In all reinforcement interventions the design must be based in the safety assessment of the actual structure, which requires the knowledge of the materials mechanical characteristics. In the case of old masonry buildings an architectural heritage

---

[1] Researcher, ICIST, IST, Technical University of Lisbon, E-mail: milosevic.m.jelena@gmail.com
[2] Assistant Professor, ICIST, IST, Technical University of Lisbon, E-mail: gago@civil.ist.utl.pt
[3] Assistant Professor, ICIST, IST, Technical University of Lisbon, E-mail: mlopes@civil.ist.utl.pt
[4] Associate Professor, ICIST, IST, Technical University of Lisbon, E-mail: rbento@civil.ist.utl.pt

value may be present and in these cases the structural rehabilitation must be designed to "keep the intervention to the minimum necessary to guarantee safety" [1]. In other hand, the design of reinforcement interventions should be based on a "full understanding of the structural behavior and material characteristics" [1].

The shear behavior of rubble stone masonry walls is an important feature for the seismic strength of old buildings, but until now few experimental tests have been done to assess the correspondent mechanical parameters. In what concerns Lisbon old buildings, the masonry mechanical characteristics of are not fully known and experimental tests are required. This paper describes the experimental and the numerical studies carried out to evaluate the shear strength of old Lisbon's buildings masonry walls.

For the experimental program four rubble stone masonry walls (120cm×120cm×70cm) were built using traditional techniques and materials. Two types of mortar were used: air lime mortar (in two masonry specimens) and hydraulic lime mortar (in the other two specimens). The specimens were tested under diagonal compression following, as close as possible, the test specifications of ASTM E519-02 standard [2] and similar works where rubble stone masonry walls were tested [3, 4]. From the tests results it was obtained for the rubble stone masonry (with air or with hydraulic lime mortar) the resistance in the absence of axial compression (cohesion) and the shear modulus.

The experimental tests were also simulated by nonlinear finite element models [5] and distinct element models [6], which provided calibration data for numerical models. The numerical models and its results, which showed a good agreement with the experimental data, are presented in the paper, as well as, some conclusions about numerical modeling strategies.

2. EXPERIMENTAL WORK

The experimental prototypes were built in laboratory using traditional techniques and intend to represent traditional masonry walls. As mentioned four masonry specimens were built: two with hydraulic mortar (W1 and W4) and two with air lime mortar (W2 and W3) and tested by diagonal compression test. The diagonal compression tests were performed to determine the diagonal tensile (shear) strength and the shear modulus of the four masonry specimens.

2.1 Diagonal compression test

The test setup is composed of two steel loading shoes, which were fixed on two opposite corners of a diagonal of the masonry specimens. On the loading shoe, which was placed on the top of the specimen, the load is applied to the panel by a hydraulic jack and transferred to the other shoe at the bottom corner, as in shown in Fig.1.
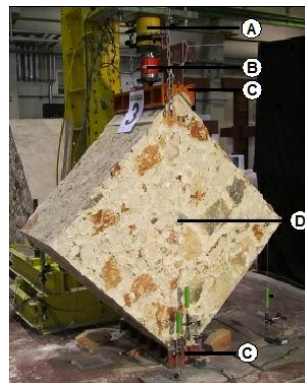

Fig. 1 Test setup for diagonal compression test
A – Hydraulic jack; B – Load cell; C – Loading shoes; D – Masonry specimens

Both sides of the specimens were instrumented with linear voltage displacement transducers (LVDT´s TSV and TSH, respectively) in order to measure shortening of the vertical diagonal and the lengthening of the horizontal diagonal. The total number of channels used for each specimen was eight: five transducers were on one side and three transducers were on the other side of the specimen, as can be seen in Fig. 2. It is worth noting, that one more transducer was placed under the hydraulic jack to measure the vertical displacement. In order to avoid damages on the instrumentation, all transducers were removed (except the one under the hydraulic jack), when the specimen showed signals that it could be close of failure. After removing the transducers, the load was continuously applied until the specimen's collapse.
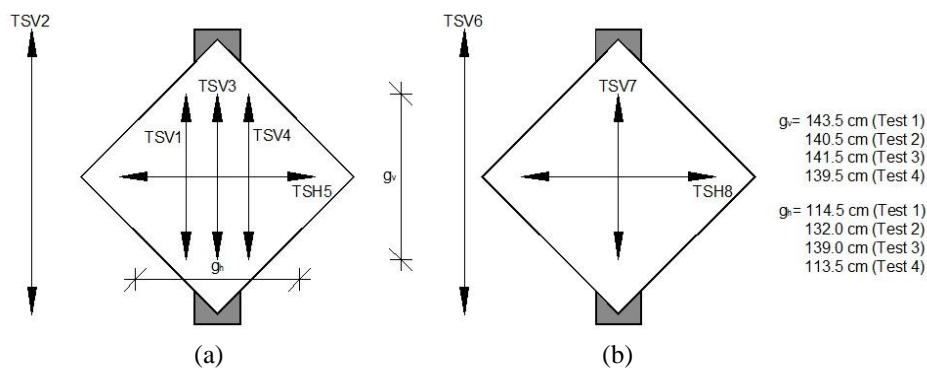

g_v= 143.5 cm (Test 1)
140.5 cm (Test 2)
141.5 cm (Test 3)
139.5 cm (Test 4)

g_h= 114.5 cm (Test 1)
132.0 cm (Test 2)
139.0 cm (Test 3)
113.5 cm (Test 4)

(a)   (b)

Fig. 2 Position of transducers: (a) wall front side; (b) wall back side (dimension in [cm])

Following the ASTM E519-02 [2] standard, the shear stress τ and the shear elastic modulus G for masonry specimens can be evaluated from the experimental results. If it is assumed that the Mohr's circle is centered in the origin of the Cartesian system of axis, the value of the shear stress τ is equal to the principal tensile stress f_t and can be obtained by:

$$\tau = \frac{0.707 \times P}{A_n} \tag{1}$$

where P is the load applied by the jack and A_n is the net area of the specimen, calculated as follows:

$$A_n = \left(\frac{w+h}{2}\right) \times t \times n \tag{2}$$

where w is the specimen width, h is the specimen height, t is the thickness of the specimen and n is the percentage of the unit's gross area that is solid, expressed as a decimal. In the present work the value $n = 1$ was adopted.

Consequently, the shear strength τ_0 (f_{v0} according to Eurocode 6 [7]) and the tensile strength are defined as:

$$\tau_0 = f_t = \frac{0.707 \times P_{max}}{A_n} \tag{3}$$

where P_{max} is the maximum load applied by the jack.

The shear elastic modulus G is obtained by:

$$G = \frac{\tau_{1/3}}{\gamma_{1/3}} \tag{4}$$

where $\tau_{1/3}$ is the shear stress for a load of 1/3 of the maximum load P_{max} and $\gamma_{1/3}$ is the corresponding distortion.

2.2 Experimental results

2.2.1 Masonry specimens based on the air lime mortar

In Fig. 3 the force-vertical displacement diagrams (where the vertical displacement represents average values of the measurement recorded using LVDTs 3 and 7), for the specimens built with air lime mortar can be seen. The ultimate load for specimen W2 was 29.1 kN with a vertical shortening of 1.58 mm (Point 1), and for the specimen W3 the ultimate load was 28.1 kN with a vertical displacement of 1.52 mm (Point 2). As referred, all transducers (except the transducers placed under the hydraulic jack) were removed before the end of the test. The dotted parts of the curves in Fig. 3 and Fig.4 (which is shown below) were obtained using the measurement of the transducers under the hydraulic jack, instead of the average values of all measurement.
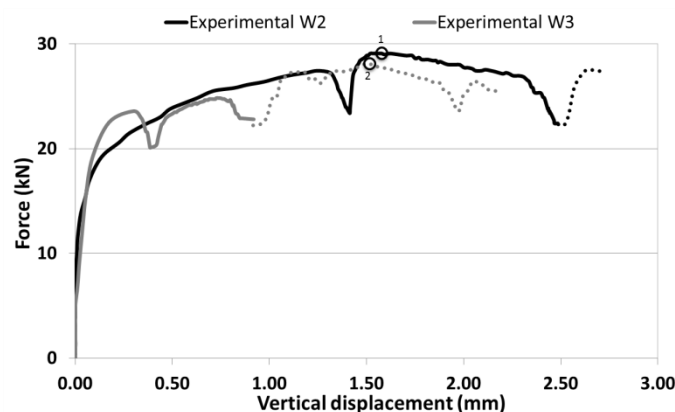

Fig. 3 Specimens W2 and W3: Force vs. Vertical displacement (Note: vertical displacement measured at the top of the specimens)

2.2.2. Masonry specimens based on the hydraulic mortar

As expected, the specimens based on hydraulic mortar showed much greater strength, comparing with specimens with air lime mortar. Namely, the maximum load for specimen W1 was 372.1 kN, with vertical shortening of 1.55 mm (Point 1). The collapse occurred later, with a load of 267.99 kN and vertical shortening of 5.29 mm (Point 2). Regarding the specimen W4, the maximum load which was applied, at the point of the collapse, was 306.24 kN, with vertical displacement of 3.47 mm (Point 3). The force-vertical displacement diagrams (where vertical displacement represents average values of the measurement recorded using LVDTs 3 and 7) for both specimens (W1 and W4) can be seen in Fig. 4. The specimen W1 was built with horizontal stone layers (at 45° to the external inclined surfaces), while the other three specimens were built with diagonal layers (45°) and this can be the reason for the most ductile behavior of the specimen W1.
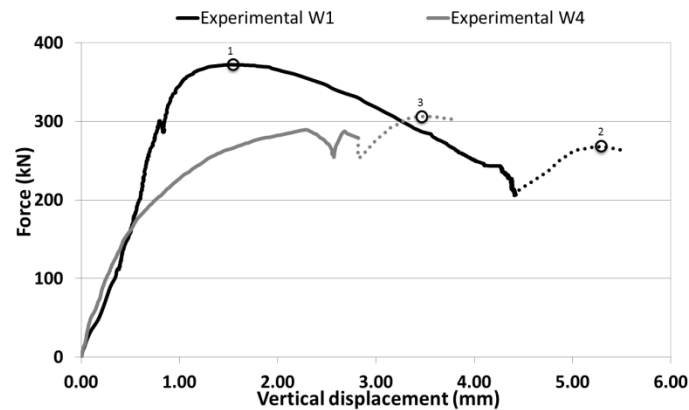
Fig. 4 Specimens W1 and W4: Force vs. Vertical displacement (Note: vertical displacement measured at the top of the specimens)

The results for all masonry specimens can be seen in Table 1.

Table 1 Results of Diagonal compression tests

Masonry typology	Masonry specimen	P_{max} [kN]	$\tau_0 = f_t$ [MPa]	G [MPa]
Rubble stone masonry specimens	W1	372.1	0.313	389.3
	W2	29.1	0.024	57.9
	W3	28.1	0.024	92.5
	W4	306.2	0.258	252.0

2.2.3 Failure modes

According to the experimental results, all tested specimens (W1, W2, W3 and W4) were characterized by similar failure patterns. In Fig. 5 the failure pattern of one specimen with air lime mortar (W3) and one with hydraulic mortar (W4) can be seen. In all tests the diagonal cracks first opened in the middle of the specimens and then extended towards the corners. None of these cracks passed through the stones and the cracks appeared only through the mortar, dividing the specimens in almost two symmetrical parts.

(a)   (b)

Fig. 5 Main crack at the middle of the specimens: (a) specimen W3 and (b) specimen W4

The specimen's collapse was fragile in cases W2, W3 and W4, but more ductile in the case of specimen W1, showing that the stone arrangement may influence the behavior. The specimens also showed different behavior after the collapse due to the different mechanical properties of mortars.

Namely, the air lime mortar specimens, W2 and W3, disintegrated after the collapse, while the specimens with hydraulic mortar, W1 and W4, divided in the two broken parts, as presented in Fig. 6.

(a)	(b)

Fig. 6 Collapse of masonry specimens: (a) specimen W3 and (b) specimen W4

2.2.4 Discussion of the experimental results

As referred, there is a difference in results between specimens W1 and W4, which were built with different stone arrangement. That outcome and the similarity of results of specimens W2 and W3, built with the same stone arrangement, indicates that the stone arrangement has influence on strength and deformation capacities of the rubble stone masonry.

Regarding the results of the by diagonal compression tests, it can be concluded that the influence of the type of mortar is very high, considering that the specimens with hydraulic mortar have shear strength 10 times higher than the specimens built with air lime mortar. Furthermore, the values obtained for shear modulus G (G was measured at 1/3 of the maximum load) also vary depending of the type of mortar. As can be seen in Table 1 the shear modulus of the air lime mortar specimens is smaller than the shear modulus obtained for the specimens made with hydraulic mortar. The shear modulus values also present a big variation between the specimens built with the same type of mortar. The variation of shear modulus (G) for air lime mortar specimens is about 38% and 35% for hydraulic lime mortar specimens. This variation can be explained by the fact that the shear modulus is evaluated on the undamaged stage, with small displacements, where measurement errors may have an important influence. The variation of the shear modulus G between specimens with hydraulic lime mortar can also be explained by the different stone arrangement adopted (W1 with horizontal and W4 with diagonal layers).

3. NUMERICAL ANALYSIS

The values of the mechanical parameters obtained by experimental tests cannot be directly used in numerical modeling. A calibration process should be done to validate the values adopted for the mechanical parameters as well as the numerical models. There is not much information about old masonry buildings mechanical parameters, but even less with regard to its use in numerical models. In this work two types of numerical models were used to simulate the diagonal compression tests described in the present paper, nonlinear finite element models [5] and distinct element models [6].

3.1 Finite Element Models

In the case of rubble stone masonry walls, the place of the potential cracks cannot be defined in advance and thus the use of the smeared crack approach in finite element models is much better and more applicable for engineering practice, comparing to the distinct crack approach.

A smeared crack model based on a fixed stress-strain concept was used (Total Strain Crack Model – [5]). In this model, the crack orientation is kept constant during the whole computation process, which is physically realistic in the current case of study. Nonlinear geometric effects were not considered in the numerical simulations and eight-node isoparametric plane stress elements (0.05m×0.05m) were used in the mesh generation.

The mechanical properties needed to describe the smeared crack model are the density (ρ =1835 kg/m^3), the Young modulus (E = 3.27 GPa), the Poisson's ratio (ν = 0.20), the tensile strength (f_t = 0.15 MPa for hydraulic lime mortar specimen or f_t = 0.01 MPa for air lime mortar specimens), the fracture energy (G_{f1} = 100 N/m) and the shear retention factor (β = 0.1). All parameters were adopted according to other works [8, 9, 10] and by calibration of the experimental and numerical results. In the numerical model the vertical load was applied monotonically at the top of the specimen and a Newton-Raphson iteration procedure was used with displacement control.

The comparison between the experimental "force-displacement" diagram (for walls with air lime and hydraulic lime mortars) with the numerical results obtained by finite element method, reveals that a reasonable matching was obtained between ultimate load and the loading branch, (see Fig. 7 and Fig. 8). Concerning the failure mode, the finite element analysis agrees reasonably well with the experimental results, for both type of mortars (Fig. 9a) b) and Fig. 10a) b)).
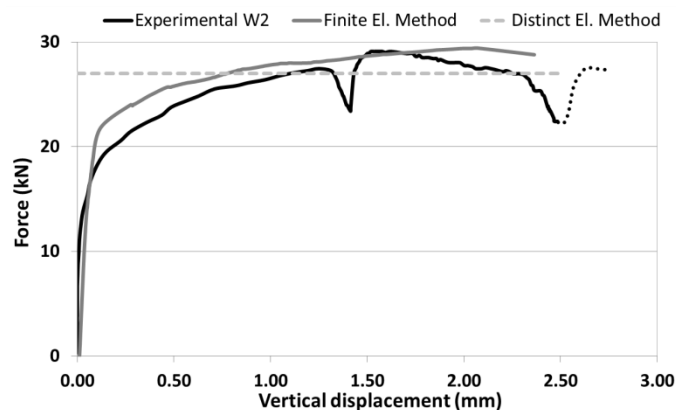

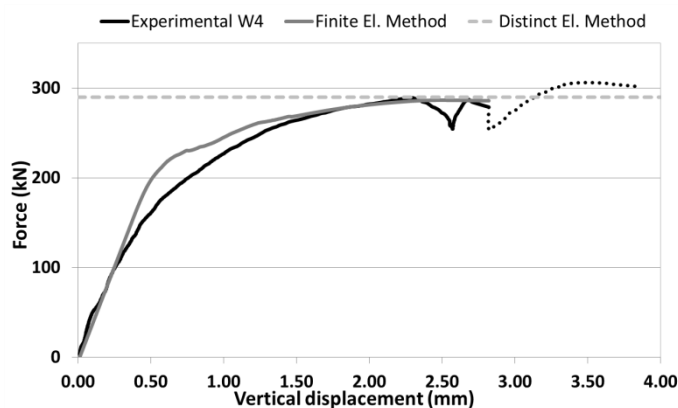Fig. 7 Experimental and numerical results: Force vs. Vertical displacement (Specimen W2)

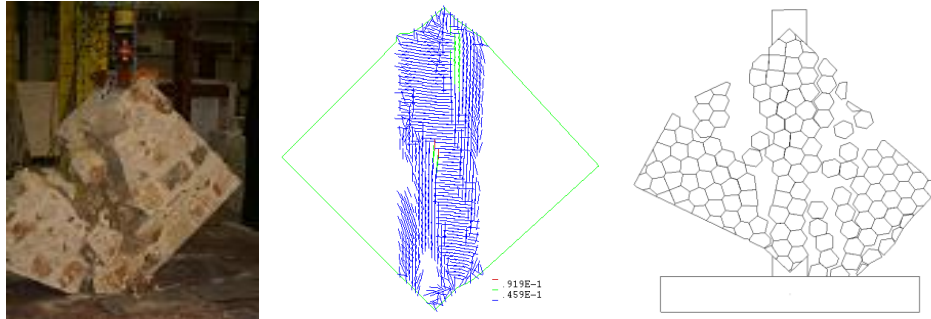Fig. 8 Experimental and numerical results: Force vs. Vertical displacement (Wall W4)

Fig. 9 Specimen W2 – Experimental and numerical failure modes: (a) Experimental; (b) Finite element model; (c) Distinct element model (specimens immediately before collapse is shown)
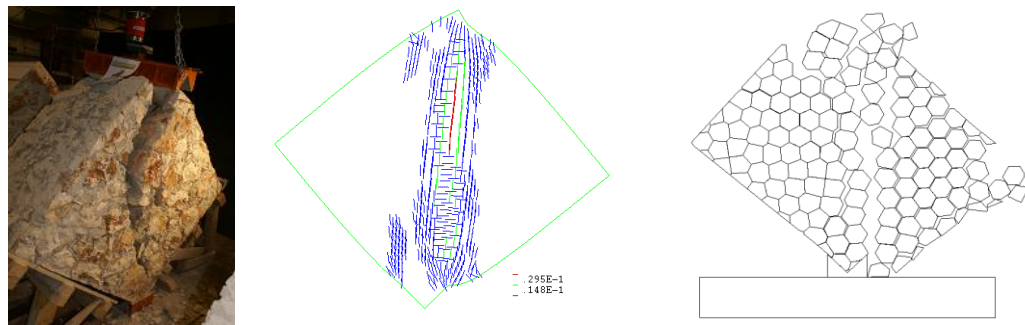

Fig. 10 Specimen W4 – Experimental and numerical failure modes: (a) Experimental; (b) Finite element model; (c) Distinct element model (specimens immediately before collapse is shown)

3.2 Distinct Element Models

The other numerical approach used to simulate diagonal compression test was the distinct element method [6]. This method allows the explicit modeling of stones and mortar joints, with displacements and rotations of the individual blocks, which allows the simulation of the failure mechanisms of stone masonry buildings. The distinct element models of the masonry specimens consisted in a group of randomly sized polygonal blocks generated by an automatic joint generator and each block simulates a stone and was modeled by a finite difference elements mesh (Fig. 11) with linear elastic behavior (bulk modulus K=410 MPa and shear modulus G=450 MPa). An appropriate behavior was assigned to the contact between the blocks using a Coulomb slip model. The parameters that control the contact behavior are the normal stiffness (J_{kn}=17 GPa and J_{kn}=8 Gpa for hydraulic and air lime mortars, respectively), the shear stiffness (J_{ks}=17 GPa and J_{ks}=8 GPa, for hydraulic and air lime mortars, respectively), the friction angle (ϕ=45º, for both type of mortars), the cohesion (c=0.23 MPa and c=0.03, for hydraulic and air lime mortars, respectively) and the tensile strength (f_t=0.23 MPa for hydraulic mortar and f_t=0.03 MPa for air lime mortar). The joint deformability parameters (J_{kn} and J_{ks}) control the initial loading branch and the joint strength parameters (ϕ, c and f_t) control the ultimate force level. All of these values were quantified based on values adopted in other works [11, 12] and on the calibration of the numerical and experimental results.
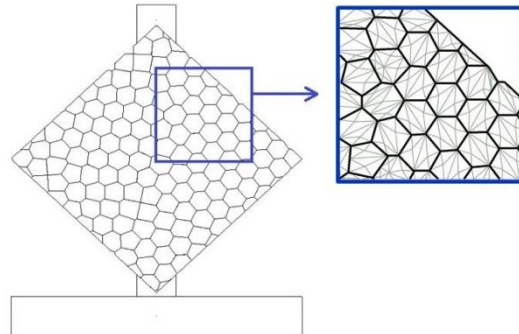
Fig. 11 Randomly sized polygonal blocks

As it can be seen in Fig. 7 and Fig. 8 a good matching between numerical and experimental values was achieved by the distinct element method for the ultimate load (for both type of walls, with hydraulic and air lime mortar). The distinct element models presented a crack pattern similar to the one developed during the experiments, for both type of mortar (Fig. 9 and Fig. 10).

3.3 Discussion of the numerical results

The numerical models, both finite element and distinct element models, showed a good matching between numerical and experimental results for the ultimate load and collapse modes. Also, the obtained failure patterns (diagonal cracking) in the numerical models were quite similar to ones seen on the experimental tests (Fig. 9 and Fig. 10). In the finite element analysis a good agreement with the experimental results was obtained for the initial branch of the "load – displacement" curve. In the distinct element analysis this curve cannot be obtained, at least not directly, which represents a clear advantage of the finite element method. However, modeling with finite element models was much more demanding in the sense that the numerical convergence required a continuous review of the convergence criteria.

4. CONCLUSIONS

For the structural assessment of old buildings with load bearing masonry walls and for the eventual design of reinforcement solutions it is required an accurate simulation of its structural behaviour. For this it is essential to know the materials mechanical characteristics, which is not always possible due to the lack of experimental data. This work aims to evaluate the shear strength for traditional rubble stone masonry walls via diagonal compression tests.

The tested masonry panels showed a fragile behavior with low values of shear strength, especially in the case of the models made with air lime mortar ($\tau_{0\ ASTM}$=0.024 MPa), as the specimens with hydraulic mortar reached $\tau_{0\ ASTM}$=0.313 MPa and $\tau_{0\ ASTM}$=0.258 MPa. It was noted that the mortar composition (air or hydraulic lime) has an important influence on shear strength. The tests showed also that an appropriate stone arrangement can increase the resistance of the wall. It can be noticed that the experimental results for shear strength obtained for specimens with air lime mortar and calculated according to the ASTM procedure ($\tau_{0\ ASTM}$=0.024 MPa) are corresponding to values of the Italian Standard [13] (τ_0==0.02 MPa to 0.032 MPa).

The tests were simulated in a numerical model by nonlinear finite elements (smeared crack concept) and distinct elements models, which demonstrated their ability to simulate the masonry behaviour in shear. Both numerical procedures gave results with a good matching to the experimental results and the collapse patterns were similar to the experimental ones. With the finite elements models the

complete load-displacement curve was obtained, whereas with the distinct element method only the maximum applied load can be obtained. However, it must be noted that in order to obtained convergence in all analysis steps, the finite element models required much more attention from the operator than in case of distinct elements models.

ACKNOWLEDGMENTS

REFERENCES

[1] ICOMOS (2003) Recommendations for the analysis, conservation and structural restoration of architectural heritage. *ICOMOS, International Scientific Committee for Analysis and Restoration of Structures of Architectural Heritage*

[2] ASTM (2002) ASTM E 519-02, Standard Test Method for Diagonal Tension (Shear) in Masonry Assemblages. *ASTM International, West Conshohocken, PA*

[3] Corradi M., Borri A., Vignoli A. (2003) Experimental study on the determination of strength of masonry walls. *Journal of Construction and Building Materials* 17(5): 325–337

[4] Brignola A., Frumento S., Lagomarsino S., Podestà S. (2008) Identification of shear parameters of masonry panels through the in-situ diagonal compression test. *International Journal of Architectural Heritage* 3(1): 52–73

[5] DIANA (2005) DIsplacement method ANAlyser, release 9.1 [CD–ROM]. *Delft, The Netherlands: TNO DIANA BV*

[6] ITASCA (2011) UDEC v4.01 - User's guide. *Itasca Consulting Group, Inc., Minneapolis,USA*

[7] EC 6 (1995) Eurocode 6 - Design of masonry structures, part 1-1: general rules for buildings – rules for reinforced and unreinforced masonry. *ENV 1996-1-1:1995*

[8] Mendes N., Lourenço P. B. (2010) Seismic Assessment of Masonry "Gaioleiro" Buildings in Lisbon, Portugal. *Journal of Earthquake Engineering* 14(1): 80-101

[9] Rots J. G., Belletti B., Boonpichetvong M., Invernizzi, S. (2006) Event by Event Strategies for Modeling Amsterdam Masonry Structures. *Structural Analysis of Historical Constructions*

[10] Ramos L.F., Lourenço P.B. (2004) Advanced numerical analysis of historical centers: A case study in Lisbon, *Engineering Structures* 26: 1295-1310

[11] Gago A. S., Alfaiate J., Lamas A. (2011) The effect of the infill in arched structures: Analytical and numerical modeling. *Journal of Engineering Structures* 33(5): 1450-1458

[12] Azevedo J., Sincraian G., Lemos J. V. (2000) Seismic behavior of blocky masonry structures. *Journal of Earthquake Spectra* 16(2): 337-365

[13] PCM 3274 (2003) Ordinanza del Presidente del Consiglio dei Ministri nº 3274, 2003: Allegato 2: - *Norme tecniche per il progetto, la valutazione e l'adeguamento sismico degli edifici, Italy*